Theoretical study on commensurability oscillation in anisotropic antidot lattices

Wenchang Lu
Max-Planck-Institut für Festkörperforschung, Heisenbergstraße 1, 70569 Stuttgart, Germany
(Received 19 March 1996)

We investigate the origin of commensurability oscillation in an antidot lattice in detail, by calculating magnetoresistance through square, rectangular, and disordered antidot lattices. Our calculations show that the commensurability oscillation in R_{xx} is mainly determined by the arrangement of antidots in the Y direction, and vice versa. In the case of a rectangular antidot lattice with $b<a$ (a and b are lattice constants in the X and Y directions), peaks in R_{xx} appear at higher magnetic fields and peaks in R_{yy} appear at lower magnetic fields. In the disorder case, X disorder suppresses the commensurability oscillation in R_{yy}, but has only a slight effect on R_{xx}. Two-direction disorder suppresses the commensurability oscillations in both R_{xx} and R_{yy}, as we expected. Our results agree quantitatively with the experiments. The electron magnetic focusing effect can be used to explain the commensurability oscillation. [S0163-1829(96)08135-0]

I. INTRODUCTION

In the last few years, weak and strong potential modulations of two-dimensional electron gas (2DEG) have been achieved in many laboratories. For the weak potential modulation, Weiss *et al.*[1] observed a type of magnetoresistance oscillation periodic in $1/B$, which is called the Weiss oscillation. For the strong potential modulation, there exists a different behavior. Weiss *et al.*[2] observed commensurability oscillations in the square antidot lattice, i.e., magnetoresistance peaks appear when the cyclotron diameter $(2R_c)$ can be associated with a commensurate orbit encircling a specific number of antidots (1,2,4,9...). The transport properties on periodic and quasiperiodic triangular antidot lattices were investigated by Takahara *et al.*,[3] and commensurability oscillations observed in their experiments. These phenomena are interpreted on the basis of pinned classical orbits in billiard model. Similar results were observed by other groups.[4]

Recent experiments by Tsukagoshi *et al.*[5] investigated the magnetoresistance through disordered and anisotropic antidot lattices in GaAs/Al_xGa_{1-x}As heterostructures, and found that the peak position in magnetoresistance depends on the current flow direction. This phenomenon cannot be interpreted by the pinned orbit model. It is suggested that the commensurability oscillations are determined only by the period along the direction perpendicular to the current.

Theoretically, Fleischmann, Geisel, and Ketzmerck,[6] using a continuous antidot potential, calculated magnetoresistance through a square antidot lattice. Their results showed that commensurability oscillations are mainly caused by the correlation function of unperturbed chaotic motion and not by the pinned orbits. Geisel, Zacherl, and Radons[7] have investigated the chaotic diffusion and $1/f$ noise of particles in two-dimensional solids, and found that the trapping mechanism no longer operates for higher energy.

To our knowledge, calculations on magnetoresistance for rectangular and disordered lattices have not been carried out. In the present paper, we study in detail the commensurability oscillation in the antidot lattice by calculating the magnetoresistance through square, rectangular, one-direction disordered and two-direction disordered antidot lattices.

Since the Fermi length λ_F is smaller than the lattice constant in the above-mentioned experiments, the problem can be dealt with in classical approximation. In Sec. II, we outline the equation of motion of the electron wave packet in the classical regime. The model potential for the antidot is also given in this section. Results and discussions on Poincaré surfaces of section and magnetoresistances are given in Sec. III and a summary is given in Sec. IV.

II. EQUATION OF MOTION AND MODEL POTENTIAL

For a perpendicular homogeneous magnetic field B, we choose the gauge

$$\vec{A}=\left(-\frac{By}{2},\frac{Bx}{2},0\right). \tag{1}$$

In the classical regime, a one-electron wave packet moving in a two-dimensional modulated potential is described by the Hamiltonian

$$H=\frac{1}{2m}\left(p_x+\frac{eBy}{2}\right)^2+\frac{1}{2m}\left(p_y-\frac{eBx}{2}\right)^2+U(x,y), \tag{2}$$

where m is the effective mass of the electron. $U(x,y)$ is the modulated potential. In the following, we measure the energy in units of E_F, the length in units of lattice constant a, the time in units of $\tau_0=(ma^2/E_F)^{1/2}$, and the magnetic field in units of $B_0=2(2mE_F)^{1/2}/ea$. When $B=B_0$, the diameter of the free cyclotron orbit equals the lattice constant a. If we define

$$v_x=\frac{1}{m}\left(p_x+\frac{eBy}{2}\right),\quad v_y=\frac{1}{m}\left(p_y-\frac{eBx}{2}\right). \tag{3}$$

Then the equation of motion can be written as

$$\dot{x}=v_x,\quad \dot{v}_x=2\sqrt{2}Bv_y-\frac{\partial U}{\partial x} \tag{4}$$

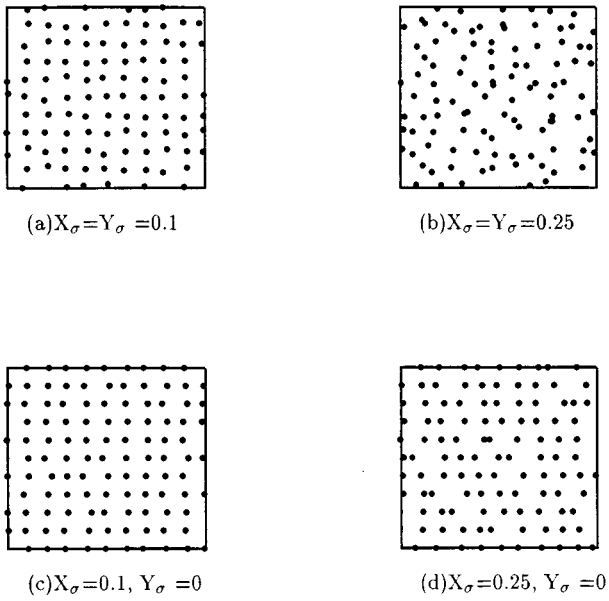

FIG. 1. The schematic view of disordered antidot lattices. Two-direction disorder with standard deviation (a) $X_\sigma = Y_\sigma = 0.1a$ and (b) $X_\sigma = Y_\sigma = 0.25a$, and one-direction disorder with standard deviation (c) $X_\sigma = 0.1a$ and (d) $X_\sigma = 0.25a$

$$\dot{y} = v_y, \quad \dot{v}_y = -2\sqrt{2}Bv_x - \frac{\partial U}{\partial y}. \tag{5}$$

Near an antidot at (x_0, y_0), the potential is modeled as an exponentially decayed function

$$U(x,y) = U_0 \exp[-\beta(x-x_0)^2 - \beta(y-y_0)^2] \tag{6}$$

where β is chosen to control the steepness of the potential, and $\beta = 320$ in the present paper. U_0 is chosen so that the potential equals Fermi energy E_F, when the distance from the center of the antidot (x_0, y_0) equals the radius of the antidot, one-sixth of the lattice constant a.

In the case of a square antidot lattice with a lattice constant a, the antidot sites $(x_0, y_0) = (na, ma)$, with n and m being integers $0, \pm 1, \pm 2, \ldots$. In the case of a rectangular antidot lattice with lattice constants a in the X direction and b in the Y direction, the antidot sites $(x_0, y_0) = (na, mb)$. When the disorder is introduced in the X direction, $x_0 = (n + \delta)a$, where δ is a random number in the Gaussian distribution with the standard deviation X_σ. When the disorder is also introduced in the Y direction, $y_0 = (m + \delta)b$. Figure 1 gives a schematic view of disordered antidot lattices with $X_\sigma = 0.1$ and 0.25, $Y_\sigma = 0$, and $X_\sigma = Y_\sigma = 0.1$ and 0.25.

III. RESULTS AND DISCUSSIONS

A. Poincaré surfaces of section

In the two-dimensional problem, the phase space (x, y, p_x, p_y) is four dimensional, and the energy surface $H = E_F$ is three dimensional. The Poincaré surface of the section at $x = x_0$ is the intersection of the energy surface with the surface $x = x_0$.[8] Since the modulated potential is periodical for the square or the rectangular antidot superlattice and quasiperiodical for the disordered antidot superlattice, it is reasonable to identify all x coordinates mod(a) and y coordinates mod(b). So, the Poincaré surfaces of the section at mod$(x,a) = 0$ reduce to a unit cell $[0,b]$ in y coordinate.

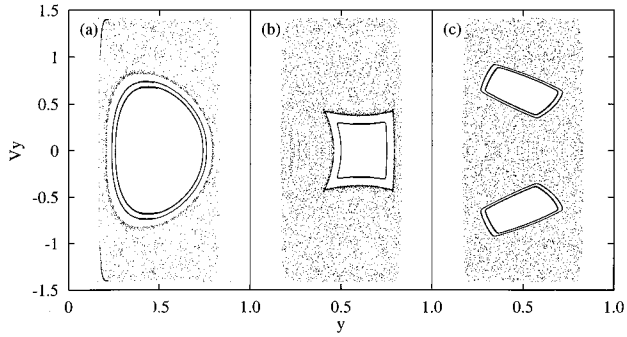

FIG. 2. Poincaré surfaces of the section in square lattice at mod$(x,1) = 0$ for (a) $B = B_0$, (b) $B = 0.8B_0$, and (c) $B = 0.45B_0$. The closed loops represent the intersections of invariant tori.

1. Square antidot lattice

Figure 2(a) shows a Poincaré surface of the section at mod$(x,a) = 0$ for the magnetic field $B = B_0$ (the diameter of the cyclotron orbit is a for this field). This Poincaré surface of the section is generated from four different initial conditions. From the figure it can easily be seen that there are a chaotic sea, a regular island near $y = 0.5$, and a line in the corner. The chaotic sea, which corresponds to the chaotic motion, is generated from one initial condition; the two closed loops in the island, which correspond to regular motion, are generated from two special initial conditions, and the line, corresponding to the drifting motion, is generated from another special initial condition.

From the Kolmogorov-Arnold-Moser (KAM) theorem,[8] the closed loop is the intersection of an invariant torus. Any orbit with a different initial condition (y, v_y) starting out on the invariant torus remains on it forever. Therefore, orbits with an initial condition (y, v_y) in the island are periodical or quasiperiodical orbits. These orbits will not drift away when a weak electric field is applied, because they circle around an antidot and are pinned by it.

The Poincaré surfaces of the section for the magnetic field $B = 0.8B_0$ and $0.45B_0$ are also shown in Figs. 2(b) and 2(c). From the calculation of the magnetoresistance below, we know that $0.8B_0$ corresponds to a valley and $0.45B_0$ to a peak in magnetoresistance. By comparing these Poincaré surfaces of the section, it can be found that the area of the regular motion island for $B = B_0$ is the largest. For this magnetic field, a large peak appears in the magnetoresistance. It is surprising that the areas of the regular motion islands for both $B = 0.8B_0$ and $0.45B_0$ are almost the same, i.e., the portions of the pinned orbits are almost the same for these two magnetic fields. But the magnetoresistance calculation shows that these two fields correspond to a valley and peak in magnetoresistance. Therefore, it may be concluded that the pinned mechanism is not the reason for the commensurability oscillation, as has been pointed out by Geisel, Zacherl, and Radons[7] and Fleischmann, Geisel, and Ketcmerick.[6]

For $B = 0.45B_0$, there are two regular motion islands. This is because the periodical orbit encircles four antidots and we

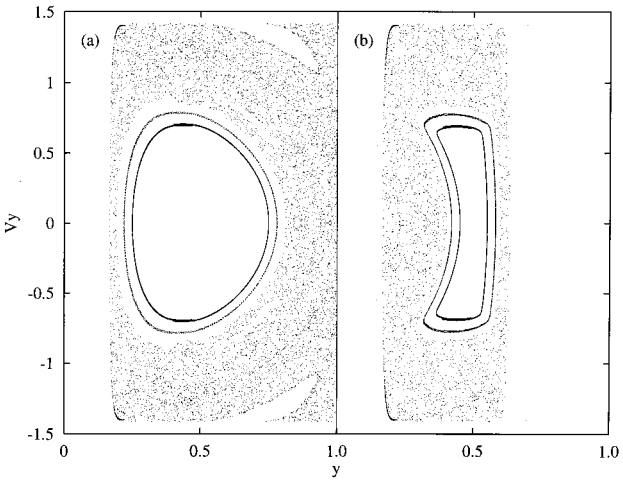

FIG. 3. Poincaré surfaces of the section in rectangular lattices (a) $b=1.2a$ and (b) $b=0.8a$ at mod$(x,1)=0$ for $B=B_0$. The closed loops represent the intersections of invariant tori. The two islands near $y=0.8a$ in (a) correspond to drifting orbits (see text).

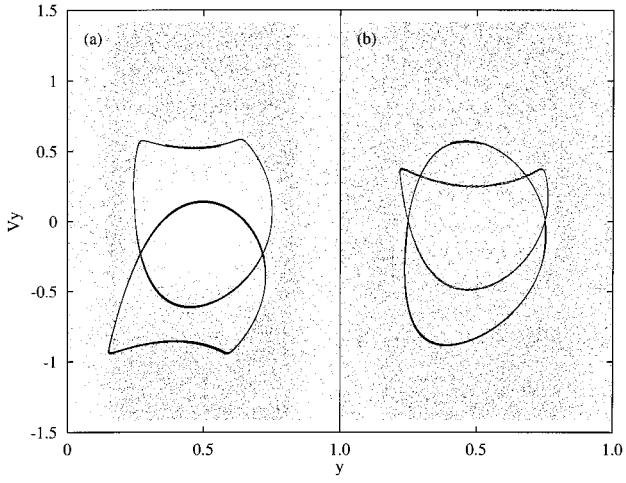

FIG. 4. Poincaré surfaces of the section in one-direction disordered lattices (a) $X_\sigma=0.1a$ and (b) $X_\sigma=0.25a$ at mod$(x,1)=0$ for $B=B_0$. The closed loops represent the intersections of invariant tori.

identify all y coordinates mod(b). For $B=0.29B_0$, there are three regular motion islands, because the periodical orbit encircles nine antidots.

2. Rectangular antidot lattice

For the magnetic field $B=B_0$, the Poincaré surfaces of the section are shown in Figs. 3(a) and 3(b) in the cases of rectangular antidot lattices with $b=1.2a$ and $0.8a$, respectively. The regular motion island in the case of $b=1.2a$ is almost the same as that for the square lattice $(b=a)$. Shapes of the closed loops are also the same as those in the case of the square lattice. But in the case of $b=0.8a$, the regular motion island is completely different from that in the case of the square lattice. The shapes of the closed loops are also different. These mean that the invariant tori in the case of $b=1.2a$ are the same as those in the case of the square lattice, and that they are different in the case of $b=0.8a$. These results can be explained as follows. The orbits on the invariant tori are cyclotronlike orbits with a radius $R_c=0.5a$. In the case of $b=1.2a$, those orbits on the invariant tori, especially on the inner ones, are almost collision free, as in the case of the square lattice. Conversely, in the case of $b=0.8a$, those orbits on the invariant tori, especially on the outer ones, are not collision free. It is obvious that the area of the regular motion island in this case is smaller than that in the case of the square lattice. This is also because some regular orbits in the square lattice change to chaotic orbits in the rectangular lattice with $b=0.8a$ due to the collision with the antidots.

For the cases $b=0.8a$, $b=a$, and $b=1.2a$, the islands of the regular motion have a fixed point at $y=0.5a$ with elliptic type. This fixed point is the intersection of mod$(x,a)=0$, with a cyclotron orbit of $R_c=0.5a$ with its center at the center of an antidot. The fixed point does not depend on the lattice constant, but on the radius of the collision-free cyclotron orbit.

In the case of $b=1.2a$, there are other regular motion islands in the Poincaré surfaces of the section (near $y=0.8a$ and $v_y=\pm 1.2$). The intersections of mod$(x,a)=0$ with these invariant tori are not closed, and the fixed point is of a hyperbolic type. According to KAM theory,[8] a hyperbolic fixed point is unstable under small perturbation. In fact, the orbit on these invariant tori is cyclotronlike, with its center near the minimum of the potential, and is not pinned by the antidot. When a weak electric field (a small perturbation) is applied, this cyclotronlike orbit will change to a drifting orbit or a chaotic orbit. Therefore, the regular orbit starting out on these invariant tori also contributes to the conductance as the chaotic orbit does.

3. One-direction disordered antidot lattice

When a fluctuation of the antidot site is introduced in one direction, for example in the X direction, the antidot lattice is disordered in this direction and ordered in the other direction. We introduce the disorder in the Gaussian distribution with a standard deviation X_σ as in the experiments by Tsukagoshi *et al.*[5] Figures 4(a) and 4(b) show Poincaré surfaces of the section for standard deviations $X_\sigma=0.1$ and 0.25, respectively. Because of fluctuation of the antidot site, there is no regular motion island, even when $X_\sigma=0.1$. But there still exist some invariant tori, whose intersections with mod$(x,a)=0$ (closed loops) are also shown in the figures. The shapes of these closed loops are different, and their fixed points are also different from one another. The reason for these results is also the fluctuation of the antidot site due to the introduction of disorder in the X direction. Orbits starting out on these invariant tori are pinned by the antidot, and they do not respond to a weak electric field, i.e., they make no contribution to the conductance.

Another difference of the Poincaré surfaces of the section in the disordered lattice from that in the ordered lattice is that chaotic orbits cover the entire Y direction [0,1]. This is because some antidots deviate from their original location in the ordered lattice, and does not mean the electron can approach the antidots.

B. Magnetoresistance

In the present classical regime, electrons with two degrees of freedom move in the three-dimensional energy surface

TABLE I. Zero-field resistances R^0_{xx} and R^0_{yy} (in units of R^0_{xx} of the square lattice) and peak positions ($2R_c$ in units of a) of P_p, R_{xx}, and R_{yy} in different cases.

	Ordered			X disordered		XY disordered	
	$b=a$	$b=0.91a$	$b=0.83a$	$X_\sigma=0.1$	$X_\sigma=0.25$	$X_\sigma=0.1$	$X_\sigma=0.25$
R^0_{xx}	1.0	1.05	1.08	1.31	1.38	2.07	2.26
R^0_{yy}	1.0	1.00	1.00	2.10	2.87	2.21	2.33
P_p	1.02	1.02	0.98	$\sim$1.0	$\sim$1.0	$\sim$1.0	
	1.58	1.49	1.45	1.56			
	2.27	2.12	2.08	2.32	2.2	2.27	
R_{xx}	1.02	0.92	0.85	1.01	1.08	$\sim$1.04	
	1.58	1.42	1.38	1.53			
	2.27	2.17	1.98	2.32	2.2	$\sim$2.22	
R_{yy}	1.02	1.02	1.02	1.04		$\sim$1.05	
	1.58	1.52	1.38				
	2.27	2.24	2.22	2.17		$\sim$2.22	

$H=E$. From the above analysis of Poincaré surfaces of the section, we know that pinned orbits starting out on the invariant tori make no contribution to the conductance. Therefore, the conductivity is the sum of contributions from chaotic orbits and drifting orbits.

According to classical linear response theory,[9] the frequency dependent conductivity at zero temperature can be written

$$\sigma_{ij}(E)=\frac{4\pi me^2}{h^2}\int_0^\infty dt e^{i\omega t}C_{ij}(t), \tag{7}$$

$$C_{ij}=\langle v_i(t)v_j(0)\rangle, \tag{8}$$

where E is the total energy of the electron, h Planck constant, and C_{ij} the velocity correlation function averaged over phase space. In the presence of impurity scattering with a mean scattering time τ, the probability that an electron is not scattered by an impurity in the time interval $[0,t]$ is $e^{-t/\tau}$. Because impurity scattering destroys any correlation, only the unperturbed orbits, which are not scattered by the impurity, make a contribution $\widetilde{C}_{ij}(t)$ to the velocity correlation function

$$C_{ij}(t)=e^{-t/\tau}\widetilde{C}_{ij}(t). \tag{9}$$

Since the contribution to the conductivity from the pinned orbits is zero, the conductivity can be written as

$$\sigma_{ij}(E)=(1-P_p)\frac{4\pi me^2}{h^2}\int_0^\infty dt\widetilde{C}_{ij}(t)e^{[-(1/\tau)+i\omega]t}, \tag{10}$$

where P_p is the portion of the pinned orbits.

The correlation function $\widetilde{C}_{ij}(t)$ can be easily obtained numerically, because it includes only the contribution from the unperturbed orbits. Then, integrating on time t, we can obtain the conductivity. At temperature T, the conductivity is finally written as

$$\sigma_{ij}=-\int_0^\infty \frac{\partial f}{\partial E}\sigma_{ij}(E)dE, \tag{11}$$

where $f=(1+e^{(E-E_F)/k_BT})^{-1}$ is the Fermi-Dirac distribution function, and k_B the Boltzman constant. In the present calculation, k_BT is chosen to be $0.007E_F$. The corresponding temperature is 1.5 K when the carrier density of the sample is 5.2×10^11 cm^{-2}. The magnetoresistances R_{xx} and R_{yy} are

$$R_{xx}=\sigma_{yy}/(\sigma_{xx}\sigma_{yy}-\sigma_{xy}\sigma_{yx}), \tag{12}$$

$$R_{yy}=\sigma_{xx}/(\sigma_{xx}\sigma_{yy}-\sigma_{xy}\sigma_{yx}). \tag{13}$$

In the case of the square lattice, R_{xx} is equal to R_{yy}. In the other cases for the rectangular and disordered lattices, R_{xx} is not equal to R_{yy}.

To calculate the magnetoresistance, it is necessary to calculate the portion of the pinned orbits first. Fleischmann, Geisel, and Ketzmerick[6] used the volume of the outermost torus in a Poincaré surface of the section to determine this portion. In the present paper, we randomly choose 6000 initial conditions in the three-dimensional energy surface, and calculate the number of pinned orbits and then the portion of the pinned orbits. Our results for the square lattice are in good agreement with those obtained by Fleischmann, Geisel, and Ketcmerick.[6] Our method is convenient, especially for the disordered antidot lattice, since it is difficult to find the outermost torus in the Poincaré surface of the section in the disordered cases. Then it is necessary to calculate the velocity correlation function. In the present paper, 6000 initial conditions are randomly chosen to make the average over phase space.

Before the discussion on magnetoresistance, it is useful to study the zero-field resistance. Table I gives the zero-field resistances R^0_{xx} and R^0_{yy} in the ordered and disordered cases. In the ordered cases, R^0_{xx} increases a little and R^0_{yy} does not change with the decrease of the lattice constant b. With the introduction of the X disorder, R^0_{yy} increases much more than R^0_{xx} does. It seems that R^0_{xx} is mainly determined by the arrangement of antidots in Y the direction, and vice versa.

First, let us consider the rectangular antidot lattice, the ordered cases. The portion of the pinned orbits P_p, and the magnetoresistances R_{xx} and R_{yy}, which are normalized to the zero-field resistances, are shown in Fig. 5 as a function of B/B_0. Peak positions appearing in these figures are listed in

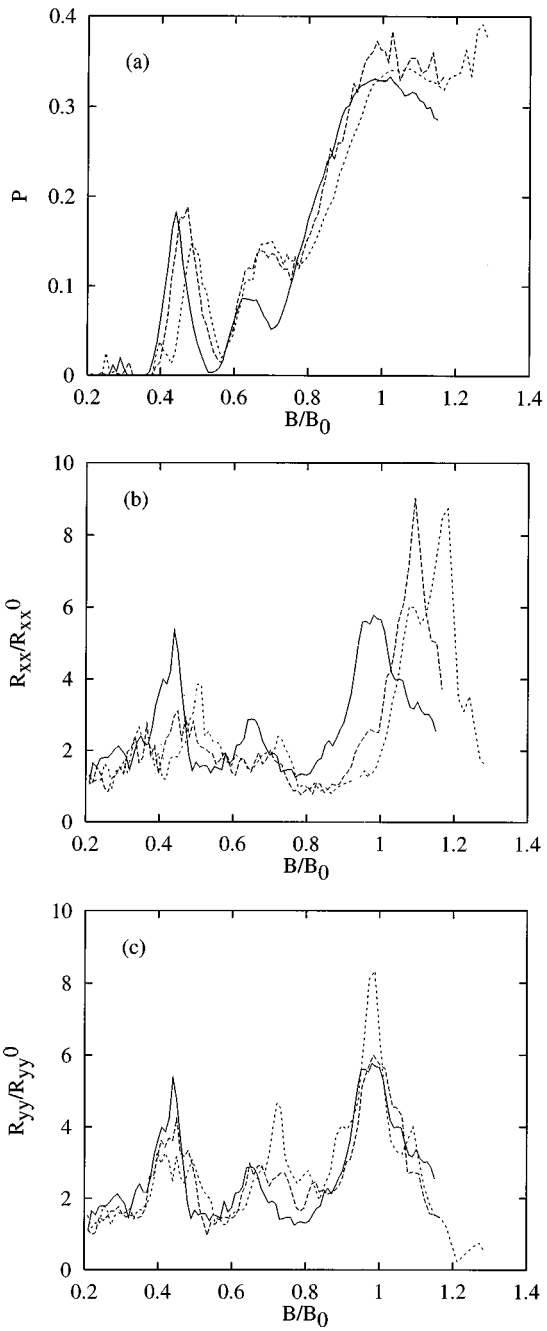

FIG. 5. (a) Portion of the pinned orbits and magnetoresistances (b) R_{xx}, and (c) R_{yy} as functions of B/B_0. Solid lines represent the case of the square lattice, and long-dashed and short-dashed lines represent the cases of rectangular lattices with $b=0.91a$ and $b=0.83a$, respectively.

Table I. The results for the square antidot lattice are also shown in these figures for comparison. As it is known, the peaks in the portion of the pinned orbits correspond to the magnetic field at which the cyclotron orbits enclose one, two, and four antidots. The peak positions shift a bit to higher magnetic fields with the decrease of the lattice constant b. The height of the peak which is related to the orbits circling around two antidots increases somewhat. The reason for this is that the corresponding radii of the cyclotron orbits become smaller and smaller with the decrease of the lattice constant b.

Comparing the peak positions in the magnetoresistance with those in the portion of the pinned orbits, one can find that they are not related, especially for the magnetoresistance R_{xx}. Therefore, the pinned orbit mechanism does not play an important role in the commensurability oscillation. The failure of the pinned orbit mechanism has also been pointed out by Geisel, Zacherl, and Radons[7] and Fleischmann, Geisel, and Ketzmerick.[6] For the magnetoresistance R_{xx}, the principal peak, at which the cyclotron motion is commensurate with the circumference around one antidot, shifts to $B\approx 1.1B_0$ and $1.2B_0$ in the cases of $b=0.91a$ and $0.83a$, respectively. The corresponding radii of the cyclotron orbits are not $0.5a$ but $0.5b$. But for the magnetoresistance R_{yy}, the principal peak does not shift in either case of $b=0.91a$ or $b=0.83a$. The second-largest peak, at which the cyclotron orbits include four antidots, tends to act in the same way as the principal peak. Experiments by Tsukagoshi *et al.*[5] observed that the peak positions depend only on the period along the direction perpendicular to the current. In other words, the lattice constant a in the X direction plays an important role in the magnetoresistance R_{yy}, and the lattice constant b in the Y direction affects mainly the magnetoresistance R_{xx}. Our calculations agree very well with their experiments.

The peak corresponding to the orbits circling around two antidots shows some different behavior from the above two peaks. For both R_{xx} and R_{yy}, this peak shifts to a higher magnetic field. In the experiment, this peak is so weak that we cannot compare it with our results. It may be because the antidot in the experiment is not so steep as the modeled potential used by us.

Second, we consider one direction disordered cases, i.e., the fluctuation of the antidot sites is introduced only in one direction, the X direction [see Figs. 1(c) and 1(d)]. The fundamental unit cell is still a square. The standard deviation X_σ is chosen to be $0.1a$ and $0.25a$ as in the experiments. Figure 6(a) gives the magnetic dependence of the portion of the pinned orbits for the cases of $X_\sigma=0$, $0.1a$, and $0.25a$. The peaks corresponding to the cyclotron orbits around one and four antidots can be clearly seen for all three cases. The peak heights decrease obviously with the increase of the standard deviation X_σ. The peak corresponding to the cyclotron orbit around two antidots disappears with the introduction of the fluctuation of antidot sites. In Sec. III A 3, we discussed the Poincaré surfaces of the section, and found that there does not exist a regular motion island for the disordered cases. But there exist some invariant tori. These results also indicate that pinned orbits exist, but the portion decreases due to the introduction of the fluctuation.

The magnetic-field dependencies of R_{xx} and R_{yy} for an X direction disordered antidot lattice are shown in Figs. 6(b) and 6(c). The curve for the square lattice ($X_\sigma=0$) is also shown in these figures. Comparing the curves for $X_\sigma=0.1a$ and $0.25a$ with the curve for $X_\sigma=0$, one can find the following facts. When $X_\sigma=0.1a$, two main peaks (circling around one and around four antidots) in both R_{xx} and R_{yy} still appear at the same magnetic field as in the square lattice. The X disorder strongly affects the peak heights of the commensurability oscillation in R_{yy}, and has only a slight effect on the peak heights in R_{xx}. When $X_\sigma=0.25a$, the commensurability oscillation in R_{yy} disappears completely. The com-

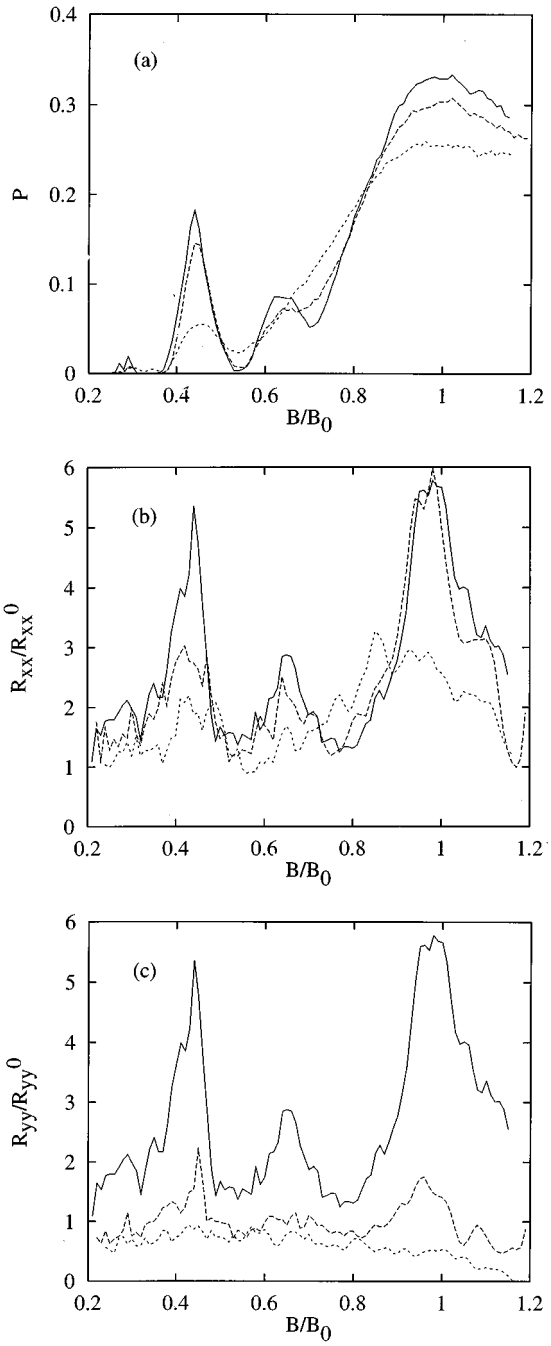

FIG. 6. The same as in Fig. 5, except that long-dashed and short-dashed lines represent the cases of one-direction disordered lattices with $X_\sigma = 0.1a$ and $X_\sigma = 0.25a$, respectively.

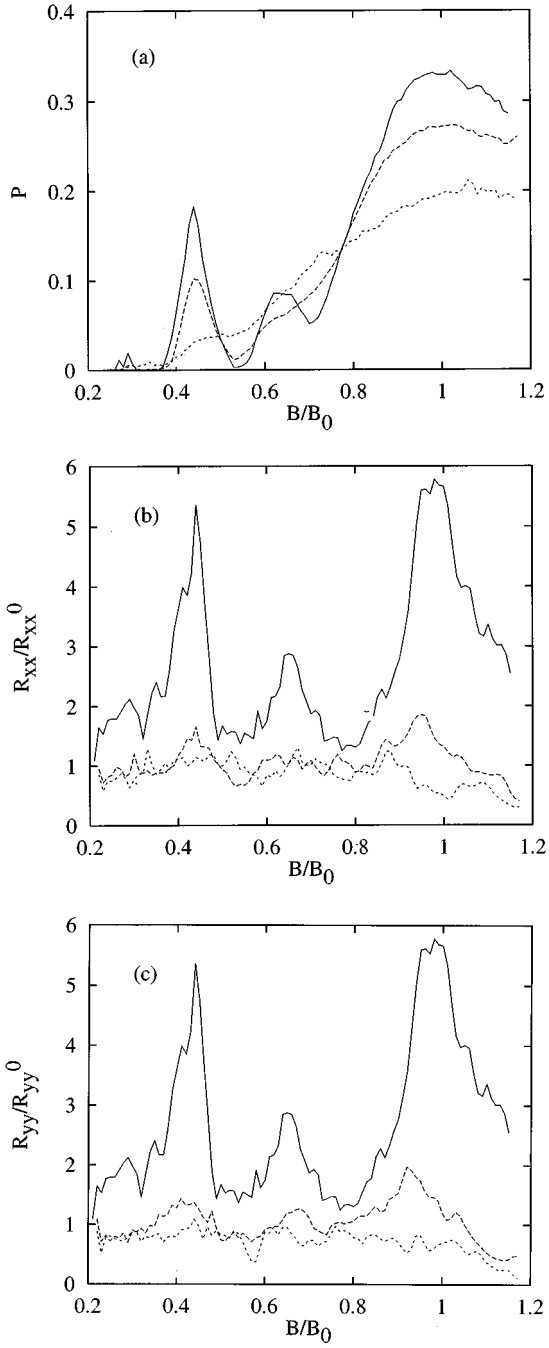

FIG. 7. The same as in Fig. 5, except that long-dashed and short-dashed lines represent the cases of two-direction disordered lattices with $X_\sigma = Y_\sigma = 0.1a$ and $X_\sigma = Y_\sigma = 0.25a$, respectively.

mensurability oscillation in R_{xx} still exists, although the peak heights decrease a great deal. The above facts indicate that the commensurability oscillation in the magnetoresistance R_{xx} depends mainly on the antidot array in the Y direction, and vice versa.

Finally, we consider two-direction disordered cases, i.e., a fluctuation of antidot sites is introduced in both X and Y directions at the same time [see Figs. 1(a) and 1(b)]. Figure 7 shows the magnetic-field dependencies of the portion of the pinned orbits P_p, and the magnetoresistances R_{xx} and R_{yy}. The portion of the pinned orbits decreases much more in two-direction disorder than in one-direction disorder. When $X_\sigma = Y_\sigma = 0.25a$, there is no peak in the curve P_p vs B/B_0. From Figs. 7(b) and 7(c), we can observe that changes in both magnetoresistances R_{xx} and R_{yy} have the same trend, because of the introduction of the fluctuation in X and Y directions with the same standard deviation ($X_\sigma = Y_\sigma$). When $X_\sigma = Y_\sigma = 0.25a$, no commensurability oscillation exists in the magnetoresistance. In other words, large fluctuations in two directions destroy all the commensurability oscillations.

Analyzing the above results for disordered cases, we can conclude that X disorder mainly affects the commensurability oscillation in the magnetoresistance R_{yy}, and destroys it when $X_\sigma = 0.25a$, and vice versa for Y disorder. Experiments[5] have observed that the peak height of the commensurability oscillation is strongly affected by the disorder in the direction perpendicular to the current. Our results are in good agreement with their experimental observations.

To sum up, there exists a commensurability oscillation in the magnetoresistance in the antidot lattice systems. What is the reason for this oscillation? Weiss *et al.*[2] suggested a pinned electron model to explain the oscillation in the square antidot lattice. Within this model, the commensurability oscillations in both R_{xx} and R_{yy} should be the same even for the rectangular or disordered antidot lattice. Theoretical studies by Geisel, Zacherl, and Radons[7] and by Fleischmann, Geisel, and Ketzmerick showed the failure of the pinned orbit explanation. The present calculations and experiments by Tsukagoshi *et al.*[5] on rectangular and disordered antidot lattice systems show the different oscillations in R_{xx} and R_{yy}, and also indicate the failure of the pinned electron model.

To understand the origin of this oscillation, let us look at experiments on the electron focusing effect. Van Houten *et al.*[10] investigated transverse electron focusing in a 2DEG, in which two point contacts were used as the injector and collector of ballistic electron. Their observation shows clearly that the electron focusing effect occurs when the separation between two point contacts is an integer multiple of the cyclotron diameter. Electrons injected from the injector can reach the collector directly or after specular reflections from the boundary. Nihey *et al.*[11] studied the magnetoresistance with multiparallel wires, and observed electron focusing effects, although the wires are longer than the ballistic mean free path. Subsequently, electron focusing effects with a single- or double-grid geometry were carried out.[12] Because of a multiple opening in the grid, i.e., multiple injectors and collectors in the grid, some peaks were observed when the cyclotron diameter is an integer multiple of the period of the grid.

The commensurability oscillation in the antidot lattice may be figured out by the idea of the electron focusing effect. An array of antidots in one direction acts as a single-grid geometry, and the antidot lattice is similar to the multigrid geometry. The lower potential region between the neighboring antidots behaves like an ''emitter'' and a ''collector'' of the electron. When the current is along the X direction, the arrangement of the antidots in the Y direction determines the separation between the ''emitter'' and ''collector.'' When magnetic fields match the separation, peaks appear in the magnetoresistance R_{xx}. Therefore, the peak positions in R_{xx} depend only on the arrangement of the antidots in the Y direction. In addition, the ballistic mean free path is affected not only by the Y-direction arrangement of antidots, but also by the X-direction arrangement. The peak heights are determined by the arrangement of antidots in both directions.

In the present antidot lattice system, the commensurability oscillation is somewhat different from that in single- or double-grid system, in which a peak appears at the magnetic field such that the diameter of cyclotron orbit is an integer multiple of the period. The diameters of cyclotron orbits corresponding to the peak positions in the present system are small (see Table I). This is due to (1) the round corner of an antidot, (2) the large gap between two neighboring antidots, and (3) scattering by the other array. In the rectangular case with $b<a$, the separation between ''emitter'' and ''collector'' in the Y direction is smaller than that in the X direction. Peaks in R_{xx} appear at higher magnetic fields, and peaks in R_{yy} appear at lower magnetic fields. In the one direction disordered case, the separation between the ''emitter'' and ''collector'' in this direction varies randomly. Therefore, the commensurability oscillation in the magnetoresistance is suppressed when the current is perpendicular to this direction. That is, the commensurability oscillation in R_{yy} is suppressed by X disorder [see Fig. 6(c) for $X_\sigma = 0.25a$], and vice versa. In the two-direction disordered case, the commensurability oscillations in both R_{xx} and R_{yy} are suppressed, as we expected.

There is an important difference in geometries between the present antidot system and the system used in magnetic focusing experiments. In magnetic focusing experiments, the geometry consists of a sequence of small constrictions separated by relatively long sections of a gate. The geometry in the present antidot lattices is, in fact, an inverse case. The width of the constrictions (about $\frac{2}{3}a$) is two times that of the gate (the diameter of the antidot is $\frac{1}{3}a$). Therefore, the magnetoresistances in the antidot lattices show some different features compared with those in the magnetic focusing experiments, i.e., the peaks in the present cases are much wider than those in the magnetic focusing experiments.

IV. SUMMARY

The motion of the electron wave packet was investigated in the classical approximation. By analyzing the Poincaré surfaces of the section, it was found that there exist regular motion islands and a chaotic sea in the case of the rectangular antidot lattice. In the case of the disordered antidot lattice, only a chaotic sea is found in the Poincaré surfaces of the section, although there still exist some invariant tori. The linear-response theory was used to calculate the magnetoresistance. In the case of the rectangular antidot lattice, the commensurability oscillation in R_{xx} is mainly determined by the period of antidots in the Y direction and vice versa. The fluctuation of antidot sites in the X direction plays only a minor role in the commensurability oscillation in R_{xx}, and plays an important role in R_{yy}. The commensurability oscillation in R_{yy} can be suppressed by the large fluctuation in the X direction. When large fluctuations is introduced in both X and Y directions, commensurability oscillations in both R_{xx} and R_{yy} are suppressed. Our results are in good agreement with experiments.[5]

The commensurability oscillations in square, rectangular, and disordered antidot lattices can be explained by the electron focusing effect. The gaps between neighboring antidots behave like an ''emitter'' and a ''collector'' of electrons. When magnetic fields match the separations between antidots, peaks appear in magnetoresistances. Because the constrictions are wider than the gates in the present antidot lattices, the peaks in the magnetoresistances are very wide. It is concluded that the commensurability oscillation can be explained by the electron focusing effect.

[1] D. Weiss, K.v. Klitzing, K. Ploog, and G. Weimann, Europhys. Lett. **8**, 179 (1989); D. Weiss, K. Richter, E. Vasiliadou, and G. Lütjering, Surf. Sci. **305**, 408 (1994).

[2] D. Weiss, M.L. Roukes, A. Menschig, P. Grambow, K.v. Klitzing, and G. Weimann, Phys. Rev. Lett. **66**, 2790 (1991).

[3] T. Takahara, T. Kakuta, T. Yamashiro, Y. Takagaki, T. Shiokawa, K. Gamo, S. Namba, S. Takaoka, and K. Murase, Jpn. J. Appl. Phys. **30**, 3250 (1991).

[4] R. Schuster, K. Ensslin, J.P. Kotthaus, M. Holland, and C. Stanley, Phys. Rev. B **47**, 6843 (1993); K. Tsukagoshi, S. Wakayama, K. Oto, S. Takaoka, K. Murase, and K. Gamo, Superlatt. Microstruct. **16**, 295 (1994); G.M. Gusev, P. Basmaji, Z.D. Kvon, L.V. Litvin, Yu.V. Nastaushev, and A.I. Toropov, J. Phys. Condens. Matter **6**, 73 (1994); G. Berthold, J. Smoliner, V. Rosskopf, E. Gornik, G. Böhm, and G. Weimann, Phys. Rev. B **47**, 10 383 (1993); R. Schuster, G. Ernst, K. Ensslin, M. Entin, M. Holland, G. Böhm, and W. Klein, *ibid.* **50**, 8090 (1994).

[5] K. Tsukagoshi, S. Wakayama, K. Oto, S. Takaoka, K. Murase, and K. Gamo, Phys. Rev. B **52**, 8344 (1995).

[6] R. Fleischmann, T. Geisel, and R. Ketzmerick, Phys. Rev. Lett. **68**, 1367 (1992).

[7] T. Geisel, A. Zacherl, and G. Radons, Z. Phys. B **71**, 117 (1988).

[8] M.V. Berry, in *Topics in Nonlinear Dynamics*, edited by S. Jorna, AIP Conference Proc. No. 46 (American Institute of Physics, New York, 1978).

[9] R. Kubo, J. Phys. Soc. Jpn. **12**, 570 (1957).

[10] H. van Houten, C.W.J. Beenakker, J.G. Williamson, M.E.I. Broekaart, P.H.M. van Loosdrecht, B.J. van Wees, J.E. Mooij, C.T. Foxson, and J.J. Harris, Phys. Rev. B **39**, 8556 (1989).

[11] F. Nihey, K. Nakamura, M. Kuzuhara, N. Samoto, and T. Itoh, Appl. Phys. Lett. **57**, 1218 (1990).

[12] K. Nakamura, D.C. Tsui, F. Nihey, H. Toyoshima, and T. Itoh, Appl. Phys. Lett. **56**, 385 (1990); Y. Hirayama and T. Saku, Phys. Rev. B **42**, 11 408 (1990); K. Nakazato, R.I. Hornsey, R.J. Blaikie, J.R. Cleaver, H. Ahmed, and T.J. Thornton, Appl. Phys. Lett. **60**, 1093 (1992).